Standard Model Highlights at ATLAS

Matouš Vozák, on behalf of the ATLAS Collaboration
Nikhef, The ATLAS experiment group, Science Park 105,
1098 XG Amsterdam, Netherlands

Over the last decades, the Standard Model (SM) has been hugely successful in describing the fundamental theory of particle interactions. The ATLAS experiment at the Large Hadron Collider (LHC) stands at the frontier of pushing the boundaries of this theory in all aspects, from precision measurements of the parameters of the SM, single and diboson production, to studying the interaction interplay of quarks inside the jets.

ATL-PHYS-PROC-2024-043
20 June 2024

1 Measurement of the W boson mass and width at $\sqrt{s}$ =7 TeV

A precise measurement of the W boson mass, m_W, and of its width, Γ_W, connected with its lifetime, is an essential test of the SM as any deviation could provide hints towards physics beyond that is contained in the SM. In the SM, m_W is closely related to other parameters via the following equation

$$m_W^2 = \frac{m_Z^2}{2}\left(1+\sqrt{1-\frac{\sqrt{8}\pi\alpha(1+\Delta r)}{G_F m_Z^2}}\right), \tag{1}$$

where m_Z is the mass of the Z boson, G_F is the Fermi constant, and α is the fine structure constant. The last term, Δr, represents loop corrections which within the SM comes mainly from heavy particles such as the Higgs boson and the top quark. Any new heavy particle X would bring an additional contribution to Δr, impacting the value of m_W. Moreover, the total width Γ_W consisting of the sum of partial widths,

$$\Gamma_W = \sum_{\ell}\Gamma_{W\to\ell\nu_\ell} + \sum_{q,q'}\Gamma_{W\to qq'} + \sum_{X}\Gamma_{W\to X}, \tag{2}$$

which represents all possible (leptonic ℓ, and quark q) decay channels of the W boson, would be also affected by additional new physics terms $\Gamma_{W\to X}$. This, together with the tension between SM and the recent CDF measurement of m_W[1], highlights the importance of the precise measurement of the W boson parameters. The ATLAS experiments focused on events where the W boson decays into a lepton and a neutrino in a special, small, subset of the data with only a low number of mean proton-proton interactions $<\mu>\sim 9$ at $\sqrt{s}=7$ TeV [2]. Both m_W and Γ_W are extracted from the simultaneous fit to the measured transverse momentum, p_{T}^{ℓ}, and transverse mass, m_{T}^{ℓ}, of the lepton in different η regions. To obtain a high precision, detailed understanding of the impact of the experimental uncertainties (electron, muon and hadronic recoil) and theoretical modelling of the measured p_{T}^{ℓ}, m_{T}^{ℓ} is paramount. Compared to the previous

analysis version on the same dataset [3], the latest ATLAS analysis improved on multiple sides of the analysis. Namely, profiling of the nuisance parameters, coming from the systematical uncertainties, was adapted in the statistical model whereas before these were computed separately. Moreover, in the fit $\Gamma_W(m_W)$ is allowed to float within the uncertainties taken from the results of the global electroweak fit [4] rather than fixed to obtain $m_W(\Gamma_W)$. Due to a strong dependence of the measurement on the parton density functions (PDFs), extensive comparison to different sets was performed and new conservative baseline PDF CT18[5] was selected. The new measured value of m_W is

$$m_W = 80366.5 \pm 9.8(\text{stat.}) \pm 12.8(\text{syst.}) \text{ MeV} = 80366.5 \pm 15.9 \text{ MeV}, \tag{3}$$

with the relative uncertainty of 0.02% making it the most precise measurement of any SM parameter at the LHC. Comparing to the previous ATLAS measurement in Figure 1 (left), the uncertainty improved by 3 MeV and the central value shifted by 3 MeV towards the SM prediction. The width of the W boson is measured to be

$$\Gamma_W = 2195.8 \pm 32.0(\text{stat.}) \pm 34.1(\text{syst.}) \text{ MeV} = 2195.8 \pm 46.8 \text{ MeV}. \tag{4}$$

As seen from Figure 1 (right), this is the most precise measurement of the Γ_W to date and lies within 2σ of the predicted SM value.

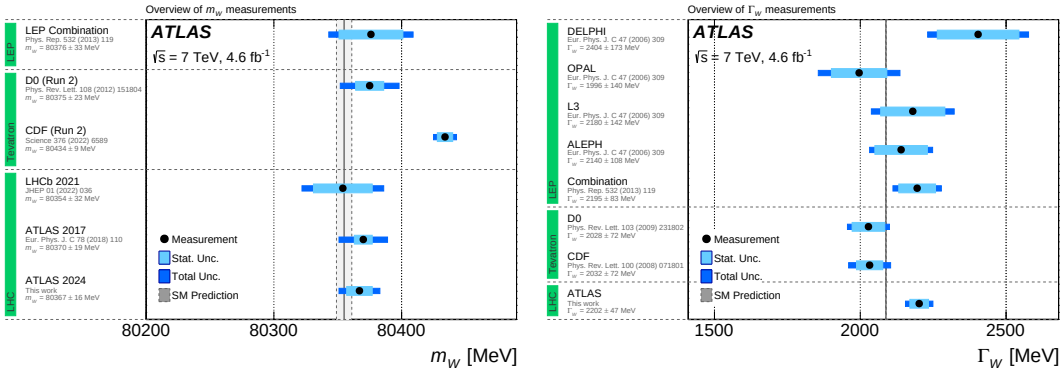

Figure 1: Overview of the measured W mass (left) and W total width (right) at LHC, Tevatron and LEP[2].

2 Measurement of W and Z boson production cross-sections at $\sqrt{s}$ =13.6 TeV

In addition to the measurement of the W boson parameters, ATLAS performed extensive validation of the SM by studying weak boson cross-sections over different centre-of-mass energies, $\sqrt{s}$, as can be seen in Figure 2 (left). The rightmost point depicts the latest measurement at 13.6 TeV using the partial Run 3 ATLAS dataset collected in 2022[6]. In addition to the total cross-section, this most recent measurement provides also fiducial cross-sections in the combined and individual flavour channels and ratios of the fiducial cross-sections, as shown in Figure 2 (right). Both ratios W^+/W^- and W^+/Z production cross-sections of weak bosons are measured to be consistent with the SM predictions and are above 1 due to the large up quark PDFs in the proton and stronger couplings of fermions to W than Z. The cross-section ratios are also made with respect to the recently measured $t\bar{t}$ production cross-section at 13.6 TeV [8] where the measured values are shifted with respect to the SM predictions by roughly 10%.

3 Measurement of WZ boson production cross-sections at $\sqrt{s}$ =13 TeV

Probing cross-sections of the diboson interactions is another important test of the SM as it stands at the core of the electroweak symmetry breaking mechanism. In particular so called

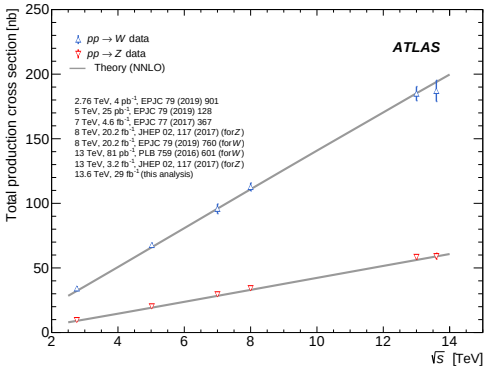

Channel	$\sigma^{\text{fid}} \pm \delta\sigma_{\text{stat}\oplus\text{syst}}$ [pb]	Acceptance A	$\sigma^{\text{tot}} \pm \delta\sigma_{\text{stat}\oplus\text{syst}}$ [pb]
$Z \to e^+e^-$	740 ± 22	0.374 ± 0.011	1981 ± 82
$Z \to \mu^+\mu^-$	747 ± 23	0.374 ± 0.011	1997 ± 82
$Z \to \ell^+\ell^-$	744 ± 20	0.374 ± 0.011	1989 ± 77
$W^- \to e^-\bar{\nu}$	3380 ± 170	0.381 ± 0.009	8880 ± 490
$W^- \to \mu^-\bar{\nu}$	3310 ± 130	0.381 ± 0.009	8680 ± 390
$W^- \to \ell^-\bar{\nu}$	3310 ± 120	0.381 ± 0.009	8690 ± 390
$W^+ \to e^+\nu$	4350 ± 200	0.366 ± 0.009	11880 ± 620
$W^+ \to \mu^+\nu$	4240 ± 160	0.365 ± 0.010	11620 ± 530
$W^+ \to \ell^+\nu$	4250 ± 150	0.366 ± 0.009	11620 ± 520
$W^\pm \to \ell^\pm\nu$	7560 ± 270	0.372 ± 0.009	20310 ± 890

Ratio	$R \pm \delta R_{\text{stat}\oplus\text{syst}}$
W^+/W^-	1.286 ± 0.022
$W^\pm/Z$	10.17 ± 0.25
$t\bar{t}/W^-$	0.256 ± 0.008
$t\bar{t}/W^+$	0.199 ± 0.006
$t\bar{t}/W^\pm$	0.112 ± 0.003

Figure 2: Summary of the W and Z total production cross-sections in ATLAS (left), summary of the individual W and Z total cross-sections, fiducial cross-sections and their ratios at 13.6 TeV (right)[6].

electroweak (EWK) production processes where vector bosons, radiated off the quarks, fuse together or scatter of each other. In addition to the EWK production, there are also interfering so called "strong" production processes as the interaction there is mediated via gluons followed by a subsequent radiation of W and Z of the quarks. The new $WZjj$ ATLAS analysis [7] utilises the full Run 2 statistics which allows to probe diboson physics differentially. Boosted decision trees (BDT) are employed to separate the EWK from the strong production process and other processes. The BDT distribution in different measured channels is then fitted to the EWK, strong and interference templates derived from the Monte Carlo predictions. Plethora of inclusive fiducial cross-sections and differential cross-sections in dijet invariant mass, number of jets ($N_{\text{jets}} = 2; >= 3$) and other kinematics such as transverse mass of WZ, m_{T}^{WZ}, are provided and compared to the predictions from the SHERPA 2.2.12 and MADGRAPH+PYTHIA 8 generators. Figure 3 (left) shows that both generators seem to over-predict the strong component particularly in the region with $N_{\text{jets}} = 2$. Fiducial cross-sections as a function of m_{T}^{WZ} are highly sensitive to the Wilson coefficients of dimension-8 EFT operators which can be seen in Figure 3 (right). The analysis provides constraints on nine independent Wilson coefficients that conserve charge conjugation and parity. The results also include the dependence of the constraints on the cut-off scale Λ.

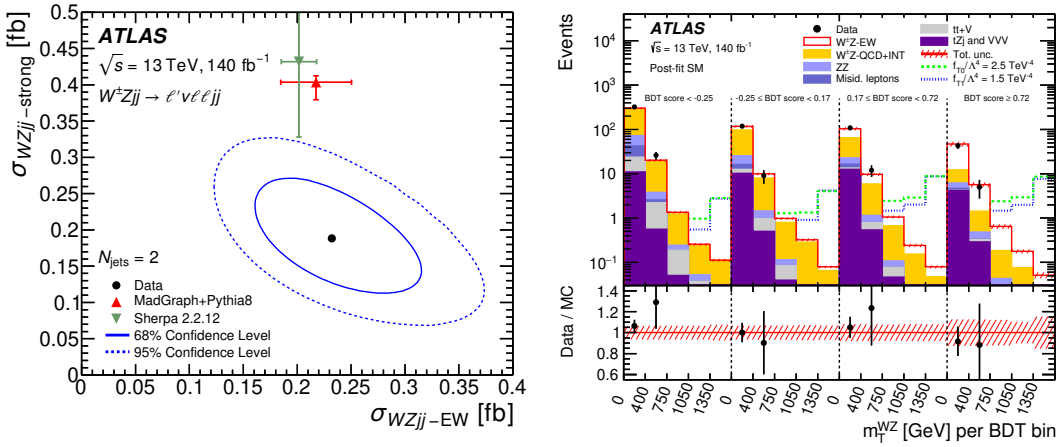

Figure 3: Contour of the strong and electroweak $WZjj$ inclusive cross-section in region with 2 jets (left), transverse mass of WZ system in different boosted decision tree bins (right)[7].

4 Jet substructures in boosted $t\bar{t}$ systems at $\sqrt{s}$ =13 TeV

Due to the nature of the strong interaction, quarks created at the LHC are always accompanied by a shower cascade of additional partons in a collimated object referred to as jet. As the energy scale of the parton splitting in this cascade gets lower, the perturbative character of the theory breaks down and phenomenological models with tunable parameters are used instead to simulate this jet substructure. It is essential to find observables that are sensitive to these parameters to constrain them from the data. Events where pairs of top quarks are produced are particularly interesting to study these observables. The recent ATLAS measurement [9] focuses on both semi-leptonic and full hadronic boosted ttbar systems using the full Run 2 dataset. In particular, the hadronic channel with a 500 GeV cut on the leading jet allows to study jet substructures in highly collimated jet configurations. The measured observables were chosen based on their sensitivity to the difference between the matrix element computation and parton shower generation, impact in the tagging algorithms, resolution and minimal correlation to the other observables. They are constructed using only track information to improve the resolution and they are unfolded to the particle level. Table 1 shows compatibility of the measured dataset with the various Monte Carlo generators in a form of the χ^2/NDF and p-values for semi-leptonic (left) and hadronic channel (right). In general 1-2 body decay observables (τ_{21}, D_2, ECF_2) with simpler jet topologies display much better description than the 3 body decay observable (τ_{32}, τ_3). Moreover, for the nominal POWHEG matrix element generator with the alternative showering using HERWIG 7 exhibits better description than PYTHIA 8. Additionally, lower final state radiation scale (FSR Down), corresponding to a higher α_S^{FSR}, seem to be preferred by the data.

Table 1: Summary tables of the compatibility of different jet substructure observables between data and various generators for the semi-leptonic (left) and full hadronic (right) channel[9].

Observable	PWG+PY8		PWG+H7		aMC@NLO+PY8		PWG+PY8(FSR Up)		PWG+PY8(FSR Down)	
	χ^2/NDF	p-value	χ^2/NDF	p-value	χ^2/NDF	p-value	χ^2/NDF	p-value	χ^2/NDF	p-value
τ_{32}	54/12	<0.01	19/12	0.09	15/12	0.24	165/12	<0.01	40/12	<0.01
τ_{21}	14/14	0.41	7/14	0.92	16/14	0.32	42/14	<0.01	8/14	0.91
τ_3	36/11	<0.01	42/11	<0.01	14/11	0.23	130/11	<0.01	23/11	0.02
$ECF2$	25/18	0.13	13/18	0.78	15/18	0.69	31/18	0.03	24/18	0.14
D_2	20/16	0.20	17/16	0.39	20/16	0.20	37/16	<0.01	15/16	0.49
C_3	11/14	0.65	6/14	0.97	3/14	1.00	35/14	<0.01	3/14	1.00
$p_{\mathrm{T}}^{\mathrm{jet}}$	27/12	<0.01	10/12	0.58	11/12	0.53	56/12	<0.01	24/12	0.02
LHA	14/17	0.65	9/17	0.92	20/17	0.29	14/17	0.69	19/17	0.32
D_2 vs. m^{top}	61/42	0.03	62/42	0.02	59/42	0.05	118/42	<0.01	44/42	0.37
D_2 vs. $p_{\mathrm{T}}^{\mathrm{top}}$	71/56	0.08	68/56	0.13	70/56	0.11	107/56	<0.01	93/56	<0.01
τ_{32} vs. m^{top}	153/42	<0.01	72/42	<0.01	56/42	0.07	413/42	<0.01	77/42	<0.01
τ_{32} vs. $p_{\mathrm{T}}^{\mathrm{top}}$	153/50	<0.01	103/50	<0.01	57/50	0.23	360/50	<0.01	114/50	<0.01

Observable	PWG+PY8		PWG+H7		aMC@NLO+PY8		PWG+PY8(FSR Up)		PWG+PY8(FSR Down)	
	χ^2/NDF	p-value	χ^2/NDF	p-value	χ^2/NDF	p-value	χ^2/NDF	p-value	χ^2/NDF	p-value
τ_{32}	24/10	<0.01	14/10	0.20	9/10	0.52	61/10	<0.01	6/10	0.82
τ_{21}	7/10	0.75	6/10	0.80	6/10	0.80	11/10	0.36	6/10	0.84
τ_3	29/7	<0.01	17/7	0.02	10/7	0.17	58/7	<0.01	8/7	0.29
$ECF2$	17/11	0.10	12/11	0.39	14/11	0.26	20/11	0.05	15/11	0.19
D_2	11/12	0.55	8/12	0.82	8/12	0.76	14/12	0.27	7/12	0.88
C_3	29/8	<0.01	21/8	<0.01	13/8	0.13	57/8	<0.01	10/8	0.28
$p_{\mathrm{T}}^{\mathrm{jet}}$	21/9	0.01	6/9	0.78	10/9	0.35	35/9	<0.01	8/9	0.54
LHA	12/12	0.49	9/12	0.74	12/12	0.46	12/12	0.43	11/12	0.53
D_2 vs. m^{top}	22/32	0.91	27/32	0.73	20/32	0.95	28/32	0.67	19/32	0.96
D_2 vs. $p_{\mathrm{T}}^{\mathrm{top}}$	29/43	0.96	26/43	0.98	28/43	0.96	32/43	0.88	26/43	0.98
τ_{32} vs. m^{top}	30/27	0.31	21/27	0.79	15/27	0.97	69/27	<0.01	11/27	1.00
τ_{32} vs. $p_{\mathrm{T}}^{\mathrm{top}}$	49/37	0.08	36/37	0.53	34/37	0.63	94/37	<0.01	30/37	0.79

5 Summary

The ATLAS experiment provides a plethora of SM measurements achieving (sub-)percent precision thanks to the continues improvements with sophisticated analysis techniques, higher order theoretical corrections, control of systematics uncertainties and larger datasets. These measurements serve as compelling evidence of the success of the Standard Model as a theory in both the electroweak and QCD sectors. Nevertheless, there are phenomena that can not be explained solely by the SM and thus new physics is needed. As such, deviations from the SM are expected and precise measurements are essential to hunt them down.

References

1. CDF Collaboration, Science 376 (2022) 170. [hep-exp]
2. ATLAS Collaboration, submitted to Eur. Phys. J. C, arXiv:2403.15085 [hep-exp]
3. ATLAS Collaboration, Eur. Phys. J. C 78 (2018) 110 arXiv:1701.07240 [hep-exp]
4. J. de Blas *et al.*, Phys. Rev. D 106 (2022) 3, 033003, arXiv:2112.07274 [hep-ph]
5. T.-J. Hou *et al.*, Phys. Rev. D 103 (2021) 014013, arXiv:1912.10053 [hep-ph].
6. ATLAS Collaboration, submitted to Phys. Lett. B, arXiv:2403.12902 [hep-exp]
7. ATLAS Collaboration, submitted to JHEP, arXiv.2403.15296 [hep-exp]
8. ATLAS Collaboration, Phys. Lett. B 848 (2024) 138376, arXiv:2308.09529 [hep-ex]
9. ATLAS Collaboration, submitted to Phys. Rev. D, arXiv:2312.03797 [hep-exp]